MRS Advances © 2019 Materials Research Society DOI: 10.1557/adv.2019.241



Electron Spin Resonance Properties of CrI₃ and CrCl₃ Single Crystals

C. L. Saiz¹, M. A. McGuire², S. R. J. Hennadige³, J. van Tol⁴, S. R. Singamaneni¹

¹Department of Physics, The University of Texas at El Paso, El Paso, Texas 79968, USA

²Materials Science and Technology Division, Oak Ridge National Laboratory, Oak Ridge, Tennessee

³Department of Chemistry, The University of Texas at El Paso, El Paso, Texas 79968, USA

⁴National High Magnetic Field Laboratory, Florida State University, Tallahassee, Florida 32310, USA

ABSTRACT

Developing functional, cleavable two-dimensional materials for use in next generation devices has recently become a topic of considerable interest due to their unique properties. Of particular interest, transition metal halides CrI₃ and CrCl₃ have shown to be good contenders for tunable and cleavable magnetic materials due to their unique magnetic properties in the monolayer. Here, electron spin resonance spectroscopy is used to pinpoint the atomic origins and underlying mechanisms of magnetic interactions as a function of temperature (5-500 K) and microwave frequency (9.43, 120 GHz) on CrI₃ and CrCl₃ bulk single crystals. ESR signals from CrI₃ due to Cr³⁺ were observed to decay at 460 K, while ESR signals from CrCl₃ remain up to 500 K. In the case of CrCl₃, the temperature dependences of signal behavior, line width and g-value show characteristic signatures of ferromagnetic fluctuations at around 40 K, near to the antiferromagnetic phase transition at 17 K.

INTRODUCTION

The discovery and subsequent research excitement of new van der Waals magnetic materials such as CrI₃ and CrCl₃ in the post silicon era offers novel applications in computing and data storage due to the unexpected magnetic properties associated with

the reduced dimension and layered structure. This is because such materials have weak van der Waals forces between layers, and therefore can be cleavable down to a monolayer where unique magnetic properties can be observed [1-3]. Particularly, the transition metal halides CrI₃ and CrCl₃ are shown to be good contenders for tunable and cleavable magnetic materials [4-6]. In these compounds, Cr3+ ions are arranged in a honeycomb network and located at the centers of edge-sharing octahedra of six halogen atoms. CrI₃ is a ferromagnet with a Curie temperature (T_C) of 61 K, while CrCl₃ is an inplane ferromagnet and out-of-plane antiferromagnet with an ordering temperature (Néel temperature, T_N) near 17 K [7-9]. The cleavable crystals are semiconducting, and because of these unique magnetic properties, are currently being actively researched for next-generation spintronic and magnetoelectronic applications [10-16]. By the nature of their crystal structures, these compounds are strongly anisotropic with magnetic behaviors determined by a weak interlayer coupling, single ion anisotropy and intralayer coupling [17]. By taking advantage of these couplings, researchers have shown that it is possible to electrically control the magnetic behavior of CrI₃ monolayer and bilayers [11].

Electron spin resonance (ESR) spectroscopy provides important information on the local magnetic nature, magnetic phase transitions and magnetic interactions in these compounds. Several decades ago, a few ESR studies conducted at and below room temperature (300 K) appeared in the literature on CrI₃ and CrCl₃ [8,18,19]. However, interest in such materials was recently rejuvenated when long-range magnetic order in pristine two-dimensional (2D) crystals Cr₂Ge₂Te₆ and CrI₃ [20], as well as the discovery of 2D ferromagnetism in the CrI₃ monolayer were first reported [10], renewing interest in compounds with similar magnetic and structural properties. In addition, to the knowledge of the authors, there have been no new reports using ESR on such compounds since 1991, where Chehab et al. studied the temperature dependence of the ESR signal coming from CrCl₃, confirming that, when a field of the order of 3000 G is applied, CrCl₃ exhibits magnetic properties characteristic of a 2D system [19]. To broaden the knowledge and understanding, in the present work, the authors studied the ESR spectral behavior above room temperature on CrX_3 (X = Cl, I) single crystals, where the magnetic field was applied within the plane of the CrX_3 layers. Here, X-band ESR (frequency, v =9.45 GHz) spectroscopy as a function of temperature from 300-500 K was employed. In addition, the magnetic phase transition in the CrCl3 compound as a function of temperature from 5-300 K at 120 GHz was studied by tracking the temperature dependences of signal behavior, signal width, and g-value (spectroscopic splitting factor). The peak-to-peak linewidth (ΔH_{pp}) of the ESR signal is directly connected to the interactions of the spins with their local environment. The change in magnitude in the gvalue (g) gives information on the atomic or molecular orbital where the unpaired electron is contained, the g-factor obtained from the resonance line reflects the strength of microscopic spin-orbit coupling. This work compares the ESR spectral properties of CrCl₃ and CrI₃ as a function of temperature and microwave frequency, which was unreported previously. The ESR findings obtained on these bulk CrX3 crystals can help in understanding the few-layer magnetism of these compounds, as it has been shown possible to infer information on single layer magnetism by ESR performed on other bulk crystals of organic layered magnets [21].

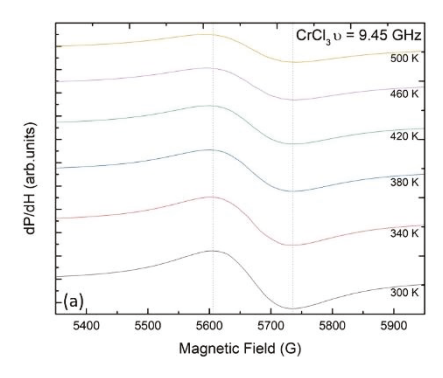
EXPERIMENTAL DETAILS

The crystals used in this study were grown by chemical vapor transport (CVT) method as described in Refs. 4 and 5. For ESR measurements, thin plate-like single crystals were wrapped in Fisherbrand $^{\text{TM}}$ pure low density PTFE tape, capable of

withstanding temperatures of -190-370 °C, inserted into 4 mm unsealed quartz tubes, and inserted into a Bruker EMXplus TM X-band ($\nu = 9.45$ GHz) ESR Spectrometer, equipped with high temperature probe head. Since the magnetic field was applied in the plane of these thin plates, the demagnetization field is negligible. High temperature (300-500 K) was controlled through the continuous flow of nitrogen gas. The complete system was operated by Bruker Xenon software. Additionally, all ESR experimental settings were kept constant for reproducibility. High frequency (120 GHz) ESR measurements were recorded at the National High Magnetic Field Laboratory (MagLab) located at Florida State University. High frequency ESR experiments are performed using the quasioptical spectrometer developed by MagLab. This setup uses a superheterodyne spectrometer, employing a quasioptical submillimeter bridge that operates in reflection mode without cavity using a sweepable 17 T superconducting magnet.

RESULTS AND DISCUSSION

Figure 1(a) shows the temperature (300-500 K) evolution of the first-derivative ESR signals collected on $CrCl_3$ single crystals measured at 9.45 GHz. At 300 K, the ESR signal is of Lorentzian shape, with an estimated g-value of 1.986 and $\Delta H_{pp} = 131$ G. These are the benchmark signatures of Cr^{3+} (S = 3/2) ions in the octahedral site where all three spins are in the t_{2g} state, which are responsible for the magnetic behavior [8,18,19]. While the ESR signal retains its shape throughout the temperature range as the temperature is increased further to 500 K, the ESR signal starts broadening linearly from 131 to 146 G. This temperature-dependent ESR linewidth in the paramagnetic phase could be due to the phonon modulation of Dzyaloshinskii–Moriya antisymmetric exchange interaction between antiferromagnetically coupled spins in $CrCl_3$. Similar behavior has been previously reported in the case of manganites [22]. As shown in Figure 1(b), the ESR signal intensity is observed to decrease as the temperature increases (Curie-type), suggesting that this compound retains its pristine paramagnetic nature even at 500 K.



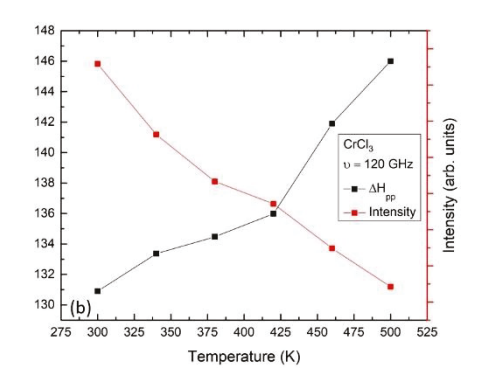


Figure 1. (a) Thermal (300-500 K) evolution of first derivative X-band (ν = 9.45 GHz) ESR signals measured on CrCl₃ single crystal. Vertical lines represent the estimation of ΔH_{pp} . (b) Signal intensity/ ΔH_{pp} vs temperature.

Temperature dependent ESR measurements were performed on CrCl₃ single crystals at 120 GHz from 5-289 K. The ESR signals as a function of temperature are

shown in Figure 2. As the sample is cooled down from 289 to 40 K, only a single Lorentzian signal with g = 1.98 and $\Delta H_{DD} = 15$ G is observed. As the sample is cooled down further, a gradual increase in the number of additional signals can be seen down to the temperature of 5 K. The temperature (~ 40 K) at which the single signal turns into multiple signals is near the magnetic phase transition at $T_N = 17$ K. This can be attributed to the fact that ESR spectroscopy is known to pick up the ferromagnetic (FM) correlations much above the transition temperature. Multiple ESR signals are typically observed in ferromagnetic compounds due to magnetocrystalline anisotropy, magnetic phase separation and magnetic inhomogeneity [23-28]. However, in the present case the former is ruled out because the magnetocrystalline anisotropy is negligible in this compound. Hence, it is most likely the local magnetic inhomogeneity that causes the multiple ESR signals due to the FM correlations that occur above the long-range antiferromagnetic (AFM) ordering temperature of this material. Upon closer inspection between 14 and 17 K, there seems to be a precursor magnetic state with some FM behavior that evolves into the AFM long-range ordering upon cooling. In this study, efforts are focused only on the signal appearing at g = 1.98 at room temperature, which persisted throughout the temperature range studied.

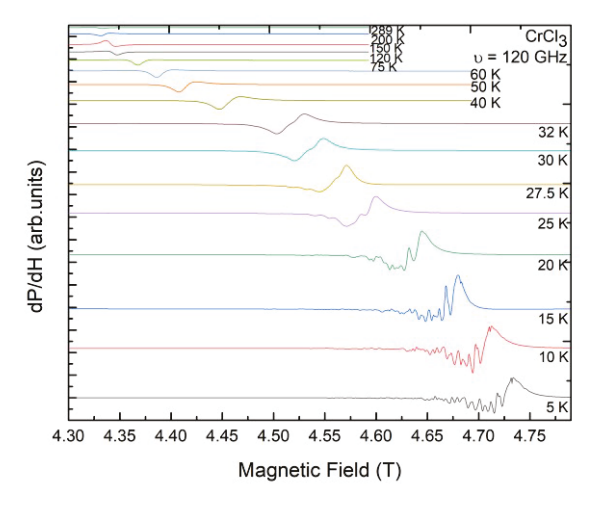


Figure 2. Temperature (5-289 K) dependence of first derivative high-frequency (v = 120 GHz) ESR signals measured on CrCl₃ single crystal.

The temperature dependence of ΔH_{pp} and g-value of this signal was tracked. The data were obtained from the fits (not shown) using a Lorentzian line shape of the signal appearing at g = 1.98 and are plotted in Figure 3. As the sample temperature is lowered from 300 K, the ΔH_{pp} begins to increase from 15 to 43 G, and starts to decrease as the temperature is lowered after about 40 K. At around the same temperature of 40 K, the g-value of the signal begins to fall sharply, possibly due to the creation of internal magnetic fields because of magnetic phase transition. This temperature is close to the AFM order (T_N) of CrCl₃. ΔH_{pp} typically linearly decreases when the temperature approaches T_N from above due to the motionally narrowed relaxation in a system with FM clusters or magnetic polarons. However, the broadening effect of ΔH_{pp} caused by the

tendency of the enhanced exchange interaction among FM clusters or the enhancement of magnetic inhomogeneity can also be developed due to the creation of internal magnetic fields with decreasing temperature [29], such as the one observed in the present work.

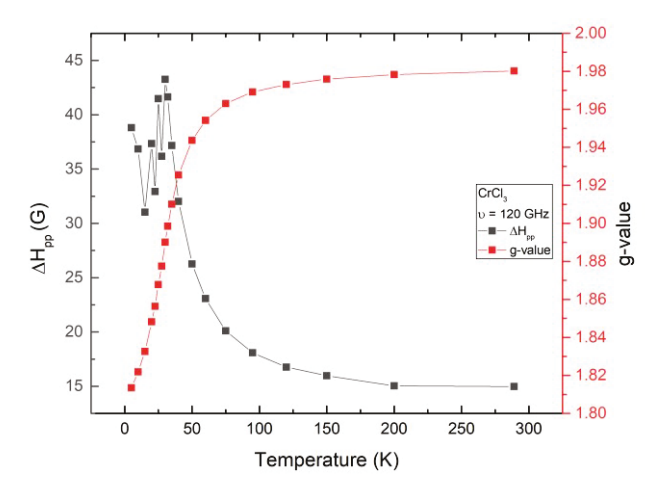


Figure 3. Temperature (5-289 K) dependences of peak-to-peak signal width (left Y-axis) and g-value (right Y-axis) extracted from the computer-generated Lorentzian fits of the high-frequency (v = 120 GHz) ESR signals measured on CrCl₃ single crystal.

High temperature ESR measurements were performed on CrI₃ single crystals. Thermal evolution of the ESR signal is depicted in Figure 4. At 300 K, the estimated gvalue from the single Lorentzian signal is 1.986 and $\Delta H_{pp} = 550$ G. As the temperature is increased, the signal is observed to broaden more than 2-times (~1250 G) at 450 K, which is much stronger than that of CrCl₃. Unlike the case of CrCl₃, the ESR signal decays as the measurement temperature increases from 300 to 450 K, and the ESR signal disappears above 450 K or broadens beyond detection limit of X-band frequency. Interestingly, at room temperature, the ESR signal appearing from CrCl₃ is narrower by a factor of four, which is a direct consequence of distinct Dzyaloshinskii-Moriya antisymmetric exchange interaction strengths between CrCl3 and CrI3 single crystals [8,18,19,22]. This observation not only confirms the presence of Cr³⁺ ions but shows the effect of halide ions (through spin-orbit coupling) on the magnetic interaction of these layered compounds, in agreement with prior studies [8,18,19]. CrI₃ is much more air sensitive than CrCl₃, and will degrade in air much more quickly, especially in moist atmosphere. At elevated temperatures, the sensitivity will be enhanced, and one would expect reaction with even a very small amount of O2 or H2O, which can make CrI3 ESRsilent. In addition, the possibility of a reaction of N₂ gas with CrI₃ at 500 K, which can also make the compound ESR-silent or change the local environment of Cr³⁺, cannot be ruled out. Further work is in progress to better understand this interesting observation.

It should be noted that in the case of CrCl₃, it is found that $\Delta H_{pp} = 131$ G at T = 300 K when measured with 9.4 GHz ESR, while $\Delta H_{pp} = 15$ G at the same temperature as measured by 120 GHz ESR. In attempting to understand the frequency-dependent linewidth, it is noted that at room temperature these compounds are paramagnets and are

therefore not expected to show magnetic relaxation effect at room temperature. The magnetic field is applied in the same way (in-plane direction) at both frequencies, hence line broadening due to the direction in which the magnetic field is applied can be ruled out. This leads to the belief that high frequency and magnetic field play a major role in the line broadening. Additional measurements are being performed at other frequencies to confirm the frequency effect on linewidth.

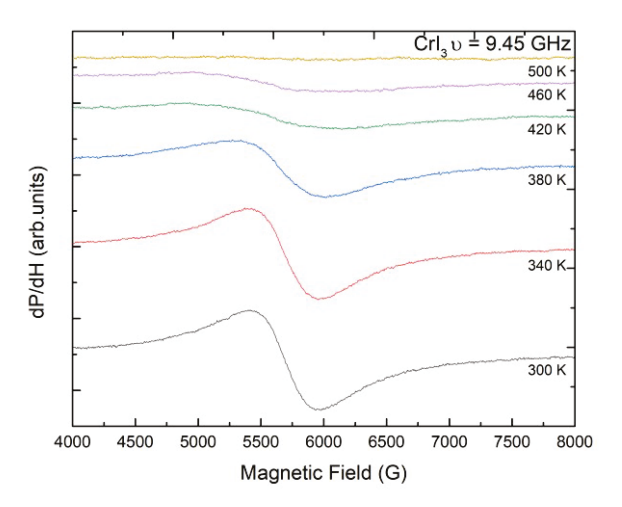


Figure 4. Thermal (300-500 K) evolution of first derivative X-band (ν = 9.45 GHz) ESR signals measured on CrI₃ single crystal.

CONCLUSION

In this paper, experimental findings on ESR investigations of CrX₃ compounds (where X = Cl, I) as a function of temperature and microwave frequency are presented. It is observed that ESR signals from CrCl₃ can be seen up to 500 K, while the signal from CrI₃, due to Cr³⁺, begins to decay at 460 K or broaden beyond the detection limit of Xband frequency above 450 K due to CrI3 becoming susceptible to decay at high temperatures. This susceptibility enhances the compound's sensitivity to very small amounts of O₂ or H₂O in the environment, which could cause CrI₃ to become ESR-silent. A reaction of N_2 gas with CrI_3 at 500 K, which can also make the compound ESR-silent or change the local environment of Cr^{3+} , is also possible. In addition, 120-GHz ESR spectroscopy was employed in order to study the magnetic correlations across the AFM phase transition in the CrCl₃ compound. The temperature dependences of signal behavior, line width and g-value show characteristic signatures of in-plane FM correlations at around 40 K, well above T_N = 17 K, which is evidence for 2D correlations developing far above the long-range ordering temperature. This study shows that ESR spectroscopy can give invaluable information on the underlying mechanisms of magnetic interactions in transition metal halides such as CrI3 and CrCl3, allowing for new opportunities in developing 2D devices for electronic applications by enabling magnetism to become a parameter that may be tunable.

ACKNOWLEDGEMENTS

This manuscript was prepared by C. L. Saiz, S. R. Singamaneni and co-authors under the award number 31310018M0019 from The University of Texas at El Paso (UTEP), Nuclear Regulatory Commission. The statements, findings, conclusions, and recommendations are those of the author(s) and do not necessarily reflect the view of the UTEP or The US Nuclear Regulatory Commission. C.L.S. and S.R.S. acknowledge support from a UTEP Start-up Grant. Crystal growth and characterization at Oak Ridge National Laboratory was supported by the US Department of Energy, Office of Science, Basic Energy Sciences, Materials Sciences and Engineering Division.

References

- 1. Cheng Gong, Lin Li, Zhenglu Li, Huiwen Ji, Alex Stern, Yang Xia, Ting Cao, Wei Bao,

- Cheng Gong, Lin Li, Zhenglu Li, Huiwen Ji, Alex Stern, Yang Xia, Ting Cao, Wei Bao, Chenzhe Wang, Yuan Wang, Z Q. Qiu, R. J. Cava, Steven G. Louie, Jing Xia & Xiang Zhang, Nat., 546, 265. (2017).
 S. Jiang, J. Shan, K. F. Mak, Nat. Mater., (2018).
 M. Bonilla, S. Kolekar, Y. Ma, H. C. Diaz, V. Kalappattil, R. Das, T. Eggers, H. R. Gutierrez, M-H Phan, M. Batzill, Nat. Nanotechnology (2018).
 M. A. McGuire, G. Clark, Santosh K. C., W. M Chance, G. E. Jellison, Jr., V. R. Cooper, X. Xu, and B. C. Sales, Phys. Rev. Mat., 1, 014001. (2017).
 M. A. McGuire, H. Dixit, V. R. Cooper, B. C. Sales, Chem. Mater., 27, 612–620 (2015).
 Wei-Bing Zhang, Qian Qu, Peng Zhua, Chi-Hang Lam, J. Mat. Chem. C 3, 12457 (2015).
 J. W. Cable, M. K. Wilkinson, E. O. Wollan, J. Phys. Chem. Solids 19, 29 (1961).
 J. F. Dillon, C. E. Olson, J. Appl. Phys., 36, 1259 (1965).
 B. Kuhlow, Phys. Stat. Sol. A 72, 161 (1982).
 B. Huang, G. Clark, E. Navarro-Moratalla, D. R. Klein, R. Cheng, K. L. Seyler, D. Zhong, E. Schmidgall, M. A. McGuire, D. H. Cobden, W. Yao, D. Xiao, P. Jarillo-Herrero, X. Xu, Nat. 546, 271 (2017).
 B. Huang, G. Clark, D. R. Klein, D. MacNeill, E. Navarro-Moratalla, K. L. Seyler, N. Wilson, M. A. McGuire, D. H. Cobden, D. Xiao, W. Yao, P. Jarillo-Herrero, X. Xu, Nat. Nanotechnology, 13, 544–548 (2018).
 D. Zhong, K. L. Seyler, X. Linpeng, R. Cheng, N. Sivadas, B. Huang, E. Schmidgall, T. Taniguchi, K. Watanabe, M. A. McGuire, W. Yao, D. Xiao, F. Jarillo-Herrero, X. Xu, Sci. Advances, 3, e1603113 (2017).
 K. L. Seyler, D. Zhong, D. R. Klein, S. Gao, X. Zhang, B. Huang, E. Navarro-Moratalla, L. Yang, D. H. Cobden, M. A. McGuire, W. Yao, D. Xiao, P. Jarillo-Herrero, X. Xu, Nat. Phys. 14, 277 (2017).
 Tong, X. Cai, M. W. Tu, X. Zhang, B. Huang, N. P. Wilson, K. L. Seyler, L. Zhu, T.

- Phys. 14, 277 (2017).

 14. T. Song, X. Cai, M. W. Tu, X. Zhang, B. Huang, N. P. Wilson, K. L. Seyler, L. Zhu, T. Taniguchi, K. Watanabe, M. A. McGuire, D. H. Cobden, D. Xiao, W. Yao, X. Xu, Science, 360, 1214 (2018).
- D. R. Klein, D. MacNeill, J. L. Lado, D. Soriano, E. Navarro-Moratalla, K. Watanabe, T. Taniguchi, S. Manni, P. Canfield, J. Fernández-Rossier, P. Jarillo-Herrero, Science, 360, 1218 (2018).
- Z. Wang, I. Gutiérrez-Lezama, N. Ubrig, M. Kroner, M. Gibertini, T. Taniguchi, K. Watanabe, A. Imamoğlu, E. Giannini, A. F. Morpurgo, Nat. Communications 9, 2516 (2018).
 L. Lado, J. Fernández-Rossier, 2D Mater. 4, 035002 (2018).
 J. F. Dillon, J. Appl. Phys., 33, 1191 (1962).
 S. Chehab, J. Amiell, P. Biensan, S. Flandrois, Physica B: Condensed Matter, 173, 211-216 (1902).

- (1991).
 20. C. Gong, X. Zhang, Science, 363, 6428, eaav4450 (2019).
 21. Á. Antal, T. Fehér, B. Náfrádi, L. Forró, and A. Jánossy, J. Phys. Society Japan 84, 124704

- A. Antal, I. Fener, B. Ivaniau, E. Forto, and (2015).
 C. Rettori, D. Rao, J. Singley, D. Kidwell, and S. B. Oseroff, M. T. Causa, J. J. Neumeier and K. J. McClellan, S-W. Cheong, S. Schultz, Phys. Rev. B 55, 3083 (1997).
 S. S. Rao, S. V. Bhat, J. Phys. D: Appl. Phys. 42, 075004 (2009).
 S. S. Rao, B. Padmanabhan, S. Elizabeth, H. L. Bhat, S. V. Bhat, J. Phys. D: Appl. Phys. 41, 155011 (2008).

- 155011 (2008).

 25. A. I. Shames, E. Rozenberg, G. Gorodetsky, A. A. Arsenov, D. A. Shulyatev, Y. M. Mukovskii, A. Gedanken, G. J. Pang, J. Appl. Phys. 91, 7929 (2002).

 26. V. Likodimos, M. Pissas, Phys. Rev. B 73, 214417 (2006).

 27. J. P. Joshi, S. V. Bhat, J. Magn. Res. 168, 284 (2004).

 28. E. A. Rozenberg, I. Shames, M. Auslender, G. Jung, I. Felner, J. Sinha, S. S. Banerjee, D. Mogilyansky, E. Sominski, A. Gedanken, Ya. M. Mukovskii, G. Gorodetsky, Phys. Rev. B 76, 214429 (2007).
- 29. A. Kiel, Phys. Rev. B 12, 1868 (1975).